Nancy Ma
e-mail: nancy_ma@ncsu.edu
Department of Mechanical and Aerospace Engineering,
Campus Box 7910,
North Carolina State University,
Raleigh, NC 27695

John S. Walker
e-mail: jswalker@uiuc.edu
Department of Mechanical and Industrial Engineering,
1206 West Green St.,
University of Illinois, Urbana, IL 61801

Laurent Martin Witkowski
e-mail: Laurent.Martin-Witkowski@limsi.fr
LIMSI,
BP133, F91403, Orsay Cedex,
France

Combined Effects of Rotating Magnetic Field and Rotating System on the Thermocapillary Instability in the Floating Zone Crystal Growth Process

This paper presents a linear stability analysis for the thermocapillary convection in a liquid bridge bounded by two planar liquid-solid interfaces at the same temperature and by a cylindrical free surface with an axisymmetric heat input. The two solid boundaries are rotated at the same angular velocity in one azimuthal direction, and a rotating magnetic field is applied in the opposite azimuthal direction. The critical values of the Reynolds number for the thermocapillary convection and the critical-mode frequencies are presented as functions of the magnetic Taylor number for the rotating magnetic field and of the Reynolds number for the angular velocity of the solid boundaries.
[DOI: 10.1115/1.1666883]

Keywords: Crystal Growth, Heat Transfer, Magnetohydrodynamics, Stability, Thermocapillary

1 Introduction

In the floating-zone (FZ) growth of semiconductor crystals, a body of molten semiconductor is held by surface tension between the melting end of a cylindrical, polycrystalline feed rod and the solidifying end of a coaxial, cylindrical single crystal. For the terrestrial, commercial FZ process, the melt zone is created and maintained by induction heating and the free surface is far from cylindrical. On the other hand, for future FZ crystal-growth experiments on the International Space Station (ISS), the free surface will be essentially cylindrical, while there will be axisymmetric radiant heating to create and maintain the melt zone. For these ISS experiments, the free-surface temperature will vary from a maximum at a middle circumference to the solidification temperature at both the feed rod and crystal interfaces. Since the surface tension of most molten semiconductors in an inert atmosphere decreases as the temperature is increased, the variations of surface tension will drive two toroidal melt circulations with flows along the free surface from the hottest circumference toward both the feed rod and crystal, and with axial return flows near the centerline. This surface-tension driven or thermocapillary convection has a very large radial derivative of the axial velocity near the free surface, and this large velocity gradient leads to a hydrodynamic instability even when the temperature difference along the free surface is quite small, e.g., 1–2°C. A much larger free-surface temperature difference is required in order to avoid the morphological instability of the crystal-melt interface which would lead to polycrystalline solidification. The thermocapillary instability involves a transition from steady axisymmetric melt motion to nonaxisymmetric steady or periodic melt motion. The quality of any semiconductor crystal depends on the uniformity of additives or dopants which give the crystal the desired electrical or optical properties. With a nonaxisymmetric melt motion, the mass transport of dopants in the melt leads to undesirable spatial oscillations of the dopant concentration in the crystal, which are called striations.

As part of the preparations for the future ISS experiments, Dold et al. [1] recently conducted terrestrial FZ experiments with radiant heating and with a small diameter for the feed rod and crystal. With this small diameter, the effects of buoyant convection and of the free-surface sag due to hydrostatic pressure were relatively small, thus roughly approximating the future experiments in microgravity. Dold et al. [1] found that the application of a rotating magnetic field (RMF) during FZ crystal growth dramatically reduced the average difference between adjacent maximum and minimum dopant concentrations in the striations. They attributed this improvement to an increase of the frequency of the periodic nonaxisymmetric thermocapillary convection. Thus in their experiments, the RMF did not eliminate the thermocapillary instability, but it reduced its deleterious effects. An RMF is produced by connecting the successive phases of a multiphase AC power source to inductors at equally spaced azimuthal positions around the melt. The inductors are generally designed to produce a spatially uniform transverse magnetic field which rotates at a constant angular velocity ω around the centerline of the melt. For the typical frequencies and field strengths used in crystal-growth experiments, an RMF produces a steady, axisymmetric, azimuthal body force on the melt. This body force drives an azimuthal velocity in the melt in the direction that the RMF rotates. If the solid boundaries are not rotating, then the axial variation of the centrifugal force due to the azimuthal velocity drives steady, axisymmetric, meridional circulations with radially inward flows near the planar liquid-solid interfaces and with radially outward flow near the plane midway between these interfaces. For the FZ process, the meridional circulations due to the RMF reinforce the thermocapillary circulations.

Walker et al. [2] recently presented a linear stability analysis for the present problem with an RMF, but without rotation of the crystal or feed rod about their common centerline. They showed that, as the strength of the RMF is increased from zero, its effects are destabilizing, i.e., the critical value of the Reynolds number for the thermocapillary convection, Re_{cr}, decreases. However, as the RMF strength is further increased, Re_{cr} reaches a minimum and then increases to values which are considerably higher than the Re_{cr} without an RMF. This stabilization emerges once the

Contributed by the Heat Transfer Division for publication in the JOURNAL OF HEAT TRANSFER. Manuscript received by the Heat Transfer Division May 23, 2003; revision received December 2, 2003. Associate Editor: V. Prasad.

azimuthal velocity produced by the RMF becomes large enough that the coupling of the radial convection of angular momentum and the centrifugal force due to the azimuthal velocity can significantly alter the base-flow thermocapillary convection.

For the FZ process, the azimuthal velocity is limited by the fact that the associated centrifugal force can overwhelm the surface tension, breaking the liquid bridge. In the FZ process, the angular velocities of the crystal and feed rod seldom exceed 30 rpm because of the free-surface stability. An RMF is also limited by the same constraint. For terrestrial FZ processes, the feed rod and crystal are often rotated with different angular velocities and in opposite azimuthal directions. However, for the future ISS experiments, the crystal and feed rod will both be clamped inside a sealed ampoule, so that only rotation with the same angular velocity and in the same azimuthal direction will be possible.

The purpose of this paper is to investigate whether combining rotation of the crystal and feed rod with an RMF can provide more stabilization of the thermocapillary convection than an RMF alone, given the constraint that the azimuthal velocity cannot exceed a certain value. If we initially apply an RMF which leads to the maximum allowable azimuthal velocity, the rotation of the crystal and feed rod in the same direction would mean that the strength of the RMF must be reduced to prevent increasing the azimuthal velocity. Thus rotation in the same direction as the RMF means reducing the stabilizing effects of the RMF, so it is not promising. On the other hand, applying an RMF in the azimuthal direction opposite to that of the crystal and feed-rod rotation might have significant effects on the thermocapillary instability without exceeding the azimuthal velocity limit. Before beginning this research, we identified a reason why this combination might be destabilizing and another reason why it might be stabilizing. Rotating the crystal and feed rod in the opposite direction from the RMF will decrease the average angular momentum. If the stabilizing effect of the RMF arises primarily from the radial convection of a strong angular momentum, then opposite rotation might be destabilizing. On the other hand, with rotation of the crystal and feed rod to produce the maximum allowable azimuthal velocity at the liquid-solid interfaces and with the RMF braking this angular velocity and possibly producing an azimuthal velocity in the opposite direction near the plane midway between these interfaces, the axial variation of the centrifugal force due to the azimuthal velocity drives two steady, axisymmetric meridional circulations with radially outward flow near the liquid-solid interfaces and with radially inward flow near the plane midway between these interfaces. These circulations tend to cancel the thermocapillary convection. Since the thermocapillary instability arises from the large radial gradient of the axial velocity near the free surface [3], the cancelation of part of the thermocapillary convection might be stabilizing. The objective of this paper is to determine whether the destabilizing effects of reduced average angular momentum or the stabilizing effects of canceling part of the thermocapillary convection dominate in this competition.

An alternative to a linear stability analysis is the time integration of the full three-dimensional governing equations. Time integrations of the full equations were presented by Rupp et al. [4] and by Fischer et al. [5] for the thermocapillary instability in the FZ process without and with an RMF, respectively. Linear stability analyses cannot be used to study nonlinear instabilities arising from finite-amplitude perturbations in the steady axisymmetric base flow. Recently Levenstam et al. [6] presented the predictions of both a linear stability analysis and of a time integration of the full three-dimensional equations for the thermocapillary instability in the FZ process, and they showed that there was good agreement between the results. This indicates that the present linear stability analysis gives accurate results for the primary transition from a steady axisymmetric flow to a periodic nonaxisymmetric flow. Many of the papers on the FZ process with an RMF were reviewed by Dold and Benz [7].

2 Problem Formulation

We assume that all the thermophysical properties of the melt are uniform and constant, except the surface tension, which decreases linearly with increasing temperature. We use cylindrical coordinates (r,θ,z) with the z axis along the centerline of the cylindrical melt zone, with the origin at the center of the melt, and with the unit vectors $(\hat{\mathbf{r}},\hat{\theta},\hat{\mathbf{z}})$. We normalize r and z with R, the radius of the melt zone, and we assume that the axial distance between the two liquid-solid interfaces is $2R$, because the height to diameter ratio of the melt zone in the actual FZ process is generally close to one.

The dimensionless governing equations are

$$\frac{\partial \mathbf{v}}{\partial t}+(\mathbf{v}\cdot\nabla)\mathbf{v}=-\nabla p+Tm f_\theta\hat{\theta}+\nabla^2\mathbf{v}, \tag{1a}$$

$$\nabla\cdot\mathbf{v}=0, \tag{1b}$$

$$\frac{\partial T}{\partial t}+\mathbf{v}\cdot\nabla T=\mathrm{Pr}^{-1}\nabla^2 T. \tag{1c}$$

The dimensionless variables t, $\mathbf{v}$, p, and T are time, the melt velocity, the melt pressure and the deviation of the melt temperature from the solidification temperature, each normalized by R^2/ν, ν/R, $\rho\nu^2/R^2$, and $(\Delta T)_c$, respectively. The dimensionless parameters here are the magnetic Taylor number $\mathrm{Tm}=\sigma\omega B^2R^4/2\rho\nu^2$, and the Prandtl number, $\mathrm{Pr}=\nu/\kappa$, where ν, ρ, σ, and κ are the kinematic viscosity, density, electrical conductivity, and thermal diffusivity of the melt, while $(\Delta T)_c$ is a characteristic temperature difference, and B is the magnetic flux density of the RMF. Assuming that the electric currents flowing through the crystal and feed rod are negligible, the dimensionless azimuthal body force due to the RMF [8] is

$$f_\theta=r-2\sum_{N=1}^{\infty}\frac{J_1(\lambda_N r)\cosh(\lambda_N z)}{(\lambda_N^2-1)J_1(\lambda_N)\cosh(\lambda_N)}, \tag{2}$$

where J_k is the Bessel function of the first kind and kth order, while λ_N are the roots of $\lambda_N J_0(\lambda_N)-J_1(\lambda_N)=0$. Equation (2) comes from a separation-of-variables solution for the electric potential function with the assumption that the melt velocity is much less than ωR. The characteristic equation for λ_N comes from the condition that the radial electric current is zero at the free surface at $r=1$ [8].

We assume that the radiant heat flux into the free surface varies parabolically from a maximum $q_{\max}$ at $z=0$ to zero at the liquid-solid interfaces at $z=\pm 1$ [4], and we use $(\Delta T)_c=Rq_{\max}/k$ for the characteristic temperature difference, where k is the thermal conductivity of the melt. Therefore the boundary conditions at $r=1$ are

$$v_r=0,\quad \frac{\partial v_\theta}{\partial r}-v_\theta+\mathrm{Re}\frac{\partial T}{\partial\theta}=0, \tag{3a,b}$$

$$\frac{\partial v_z}{\partial r}+\mathrm{Re}\frac{\partial T}{\partial z}=0,\quad \frac{\partial T}{\partial r}=1-z^2, \tag{3c,d}$$

where $\mathrm{Re}=(-d\gamma/dT)(\Delta T)_c R/\rho\nu^2$ is the Reynolds number for the thermocapillary convection, and $d\gamma/dT$ is the constant, negative derivative of the surface tension with respect to temperature. The Marangoni number used in many other studies of thermocapillary convection is equal to $\mathrm{Pr\,Re}$. The temperature term in Eq. (3b) drops out for the axisymmetric base flow, but it is important for the nonaxisymmetric perturbation. The boundary conditions at $z=\pm 1$ are $v_r=v_z=T=0$ and $v_\theta=\mathrm{Re}_\Omega r$, where $\mathrm{Re}_\Omega=\Omega R^2/\nu$ is the Reynolds number for the crystal and feed-rod rotation with the angular velocity Ω.

For each variable v_r, v_θ, v_z, p, and T, we introduce the form

$$v_r=v_{r0}(r,z)+\varepsilon\,\mathrm{Real}[v_{r1}(r,z)\exp(\lambda t-im\theta)]. \tag{4}$$

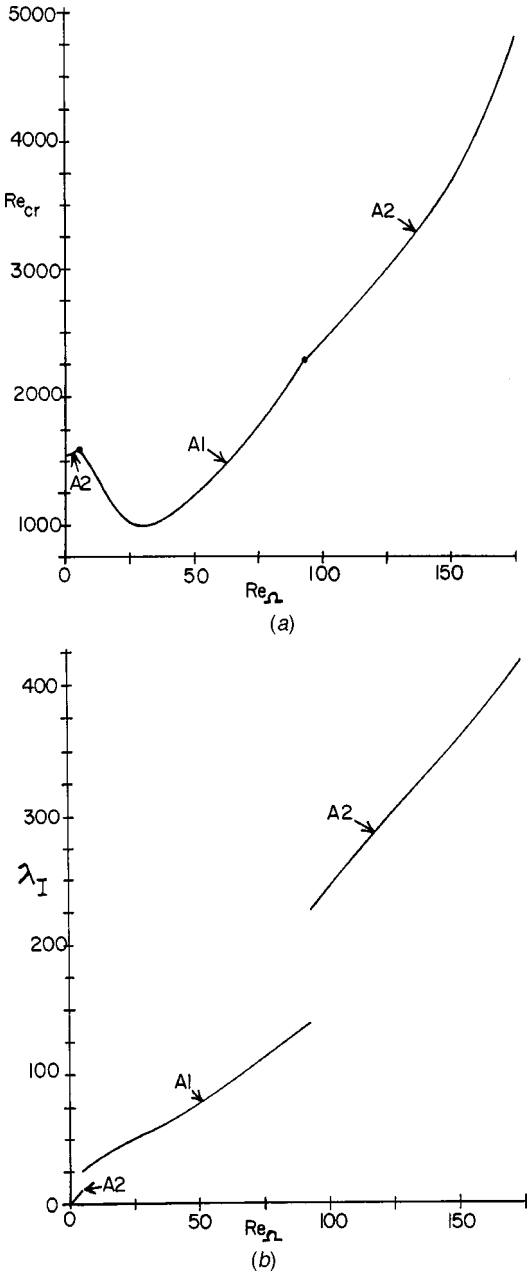

Fig. 1 Critical mode results for rotation of the crystal and feed rod without a rotating magnetic field: (a) Re_{cr} versus Re_Ω; and (b) λ_I versus Re_Ω

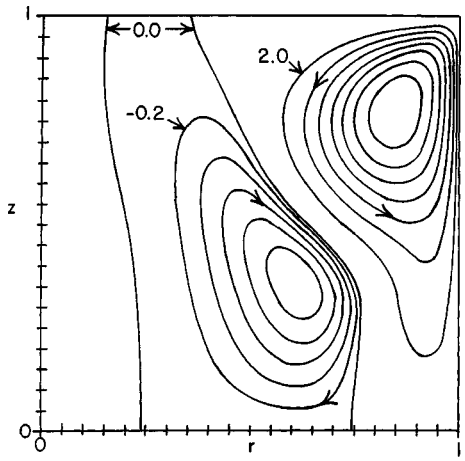

Fig. 2 Base-flow streamlines for $Tm=0$, $Re_\Omega=150$ and $Re_{cr}=3651.9$: $\psi_0=2.0k$ for $k=0$ to 7 and $\psi_0=-0.2k$, for $k=1$ to 5

The subscript 0 denotes the variables for the steady, axisymmetric base flow, the subscript 1 denotes the complex modal functions, such as $v_{r1R}+iv_{r1I}$, for the small, $O(\varepsilon)$ perturbation in the linear stability analysis, $\lambda=\lambda_R+i\lambda_I$ is the complex eigenvalue, and m is the real, integer azimuthal wave number.

For the base flow, we introduce the stream function $\psi_0(r,z)$, where

$$v_{r0}=\frac{1}{r}\frac{\partial\psi_0}{\partial z}, \quad v_{z0}=-\frac{1}{r}\frac{\partial\psi_0}{\partial r}. \tag{5a,b}$$

We eliminate p_0 by cross-differentiating the r and z components of the momentum equation (1a) for the steady, axisymmetric base flow. Since $v_{\theta 0}$ and T_0 are even functions of z, while ψ_0 is an odd function of z, we need only treat $0<z<1$ for the base flow with symmetry conditions at $z=0$. We represent each base-flow variable by a sum of Chebyshev polynomials in r and z, and we insure that the representation for each variable has the correct Taylor series in r, e.g., the Taylor series of ψ_0 has only even powers of r, beginning with r^2. We apply the governing equations and boundary conditions at the Gauss-Lobatto collocation points. We solve the nonlinear, algebraic equations for the coefficients in the Chebyshev-polynomial representations using the Newton-Raphson method [9].

Since the base flow is symmetric in z, we need only treat $0<z<1$ for the small perturbations as long as we consider both symmetric and antisymmetric modes. For a symmetric mode, v_{r1}, $v_{\theta 1}$, p_1, and T_1 are even functions of z, while v_{z1} is an odd function of z, thus matching the symmetry of the base flow. For an antisymmetric mode, v_{r1}, $v_{\theta 1}$, p_1, and T_1 are odd functions of z, while v_{z1} is an even function of z. The small-perturbation boundary value problem for $m=0$ is different and simpler compared to that for $m\geqslant 1$, so that we treat four perturbation cases: namely symmetric and antisymmetric modes with $m=0$ and $m\geqslant 1$. We represent each perturbation variable as a sum of Chebyshev polynomials in r and z, and again we insure that each representation has the correct Taylor series expansion, e.g., the Taylor series for v_{r1} for $m\geqslant 1$ has the powers $r^{(m-1)}$, $r^{(m+1)}$, $r^{(m+3)}$, ... The linear perturbation equations and boundary conditions are applied at the Gauss-Lobatto collocation points to obtain a linear, matrix eigenvalue problem. The eigenvalues are obtained with subroutines from the EISPACK library of FORTRAN codes [10].

For each set of values for Pr, Tm, Re_Ω, and Re, we first used the Newton-Raphson iteration to find the steady, axisymmetric base flow, and then we used the EISPACK subroutines to find the eigenvalues for the symmetric and antisymmetric perturbation modes for $m=0$ to 4. For each set of values for Pr, Re_Ω, and Tm, we increased Re until one eigenvalue for one mode had $\lambda_R=0$, while all the other eigenvalues for this mode and for all the other modes had $\lambda_R<0$. This defines the critical value of the Reynolds number for the thermocapillary convection Re_{cr} and the dimensionless frequency λ_I of the critical mode for a given material represented by Pr, for a given angular velocity for the crystal and feed rod represented by Re_Ω, and for a given RMF strength represented by Tm.

3 Results

We only present results for Pr=0.02, corresponding to silicon. In order to validate our code, we first treated the ''half-zone'' problem, which has been treated in a number of previous papers. For the half-zone problem, the geometry is the same, but there is no heat transfer across the cylindrical free surface and the two liquid-solid interfaces are at different temperatures, so that the free surface temperature varies from a maximum at the hotter interface to a minimum at the colder interface. We consider the

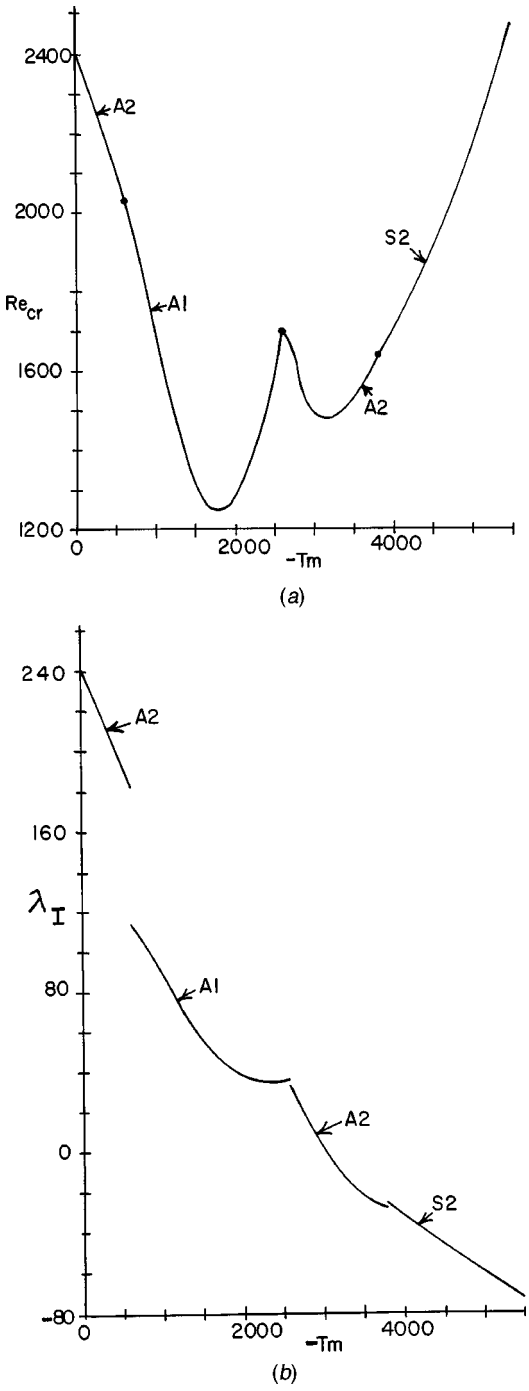

Fig. 3 Critical mode results versus $-Tm$ for $Re_\Omega=100$; (a) Re_{cr} versus $-Tm$; and (b) λ_I versus $-Tm$

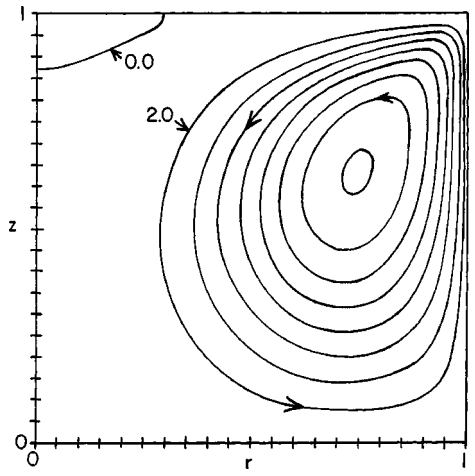

Fig. 4 Base-flow streamlines for $Re_\Omega=100$, $Tm=-5500$ and $Re_{cr}=2472.7$: $\psi_0=2.0k$, for $k=0$ to 8

half-zone problem with an axial distance between the liquid-solid interfaces equal to R, with no RMF ($Tm=0$), with no crystal or feed-rod rotation ($Re_\Omega=0$), and with $Pr=0.02$. For this case, our code gives $Re_{cr}=2059$, with $m=2$ and $\lambda_I=0$. Chen et al. [11] found that $Re_{cr}=2054$ and Wanschura et al. [3] found that $Re_{cr}=2062$, both with $m=2$ and $\lambda_I=0$.

For our FZ problem, we first consider the effects of crystal and feed-rod rotation without an RMF ($Tm=0$). The values of Re_{cr} and λ_I for $Tm=0$ and $0\leqslant Re_\Omega\leqslant 175$ are presented in Fig. 1. Here the critical mode is always an antisymmetric mode with either $m=1$ or $m=2$, denoted by A1 and A2, respectively. The meridional base flow consists of two opposite toroidal vortices with circular centerlines at some radius and at symmetric values of z. An antisymmetric $m=1$ mode represents a transition to a flow with a primary transverse vortex about a straight centerline along some diameter in the $z=0$ plane. Rupp et al. [4] found this $m=1$ antisymmetric transition to a transverse vortex with a much weaker secondary opposite vortex near one side of each liquid-solid interface. Without an RMF, they found that this pattern is stationary ($\lambda_I=0$). With an RMF, Fischer et al. [5] found that this pattern rotates in the azimuthal direction of the RMF, and they suggested that this pattern is simply convected with the azimuthal velocity produced by the RMF. An antisymmetric $m=2$ mode leads to a flow with two opposite vortices about parabolic centerlines in the $z=0$ plane and extending from the free surface at $\theta=\pm\pi/4$ through the melt and back to the free surface at $\theta=\pm 3\pi/4$. Again the pattern rotates in the azimuthal direction if there is any azimuthal base-flow velocity. The value $Re_\Omega=175$ corresponds to the kinematic viscosity of molten silicon, a diameter of 10 mm and rotation at 23.4 rpm. Dold et al. [1] grew silicon crystals with 8–14 mm diameters. The effects on Re_{cr} of rotation alone are very similar to those of an RMF alone [2]. As Re_Ω is increased from zero, the antisymmetric $m=2$ mode is stabilized until the transition to an antisymmetric $m=1$ mode at $Re_\Omega=4.724$ and $Re_{cr}=1603.4$, while λ_I abruptly increases from 11.67 to 25.07 at this switch of modes. As Re_Ω increases from 4.724, Re_{cr} decreases to a minimum of 995.0 at $Re_\Omega=30.0$ and then begins to increase. At $Re_\Omega=93.3$ and $Re_{cr}=2282$, there is a switch from the antisymmetric $m=1$ mode back to the antisymmetric $m=2$ mode, while λ_I abruptly increases from 138.8 to 226.2 at this switch of modes. At $Re_\Omega=175$, $Re_{cr}=4819.3$ and $\lambda_I=417.59$. The Re_{cr} exceeds 1547.6 when $Re_\Omega>65$, so that rotation is stabilizing for $Re_\Omega>65$. From Eq. (4), the dimensionless angular velocity of the critical disturbance is λ_I/m. For both the $m=1$ and $m=2$ antisymmetric modes, $(\lambda_I/m)>Re_\Omega$, so that the critical disturbance propagates in the direction of the crystal and feed-rod rotation with an angular velocity which is greater than Ω. The difference is larger for the $m=1$ mode than for the $m=2$ mode. For the $m=1$ mode, the ratio $(\lambda_I/m\ Re_\Omega)$ decreases from 5.3 at $Re_\Omega=4.724$ to 1.49 at $Re_\Omega=93.3$. For the $m=2$ mode, this ratio is roughly 1.2 for both $Re_\Omega<4.724$ and $93.3<Re_\Omega<175$. The fact that $\lambda_I/m>Re_\Omega$ for both modes means that the perturbation is not simply convected with the azimuthal velocity created by system rotation. Instead the perturbation propagates in the azimuthal direction because of a coupling between the centrifugal force and the radial convection of angular momentum [2].

An azimuthal base-flow velocity opposes radial velocities through the Taylor-column effect, i.e., an inward radial convection of angular momentum causes the local $v_{\theta 0}$ to increase, leading to an increase of the radially outward centrifugal force opposing the inward velocity. For $Tm=Re_\Omega=0$, the meridional thermocapillary

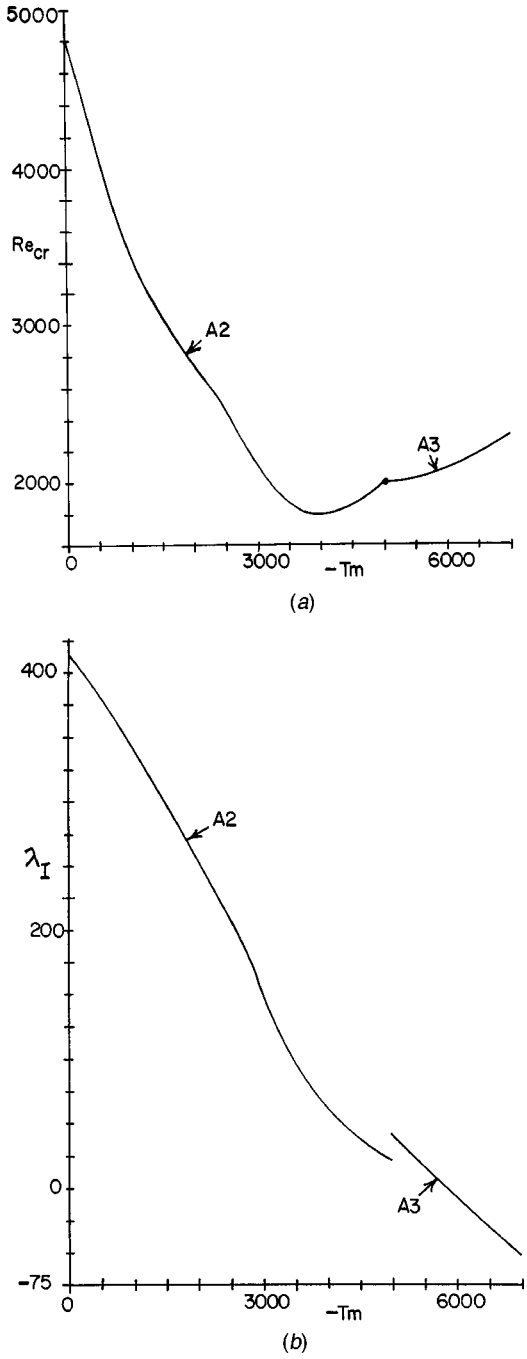

Fig. 5 Critical mode results for $Re_\Omega=175$: (a) Re_{cr} versus $-Tm$; and (b) λ_I versus $-Tm$

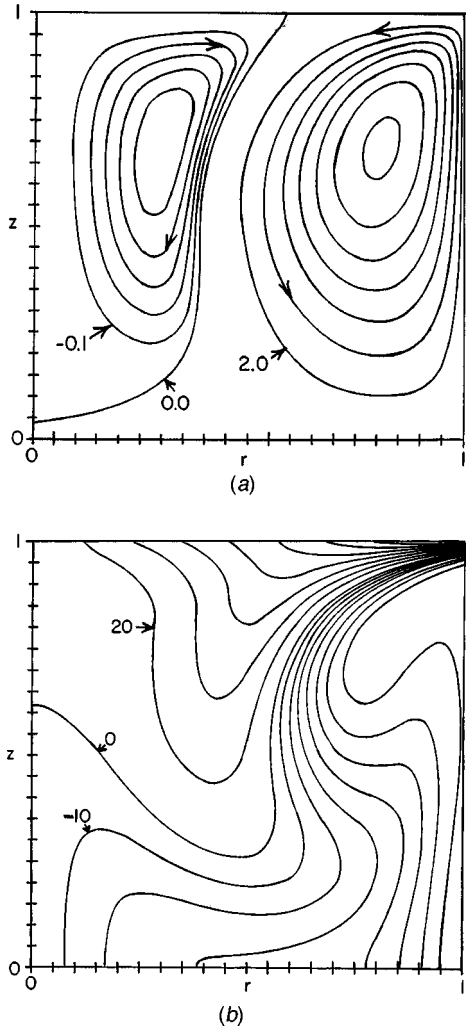

Fig. 6 Base-flow results for $Re_\Omega=175$, $Tm=-7000$ and $Re_{cr}=2297$: (a) Streamlines for meridional flow: $\psi_0=2.0k$, for $k=0$ to 7 and $\psi_0=-0.1k$, for $k=1$ to 5; and (b) Lines of constant azimuthal velocity: $v_{\theta 0}=20k$, k=0 to 8 and $v_{\theta 0}=-10k$, k=1 to 7

convection for $0\leqslant z\leqslant 1$ is a single counterclockwise circulation occupying most of $0\leqslant r\leqslant 1$. As Re_Ω is increased from zero, the Taylor-column effect opposes any radially inward flow, so that the meridional circulation is pushed toward the free surface, while the center of this circulation moves axially toward $z=1$ where the free-surface temperature gradient is largest. At roughly $Re_\Omega=40$, a second clockwise meridional circulation for $0\leqslant z\leqslant 1$ appears near $r=z=0$. This secondary circulation is driven by viscous shear from the primary circulation and by the axial variation of the centrifugal force created by the radial convection of angular momentum by the primary counterclockwise circulation. As Re_Ω is increased further, the primary counterclockwise circulation is pushed more toward the free surface, and the secondary clockwise circulation grows in magnitude and extent. At roughly $Re_\Omega=120$, a third counterclockwise circulation appears near $r=z=0$, although this third circulation is very small. The base-flow streamlines for $Tm=0$, $Re_\Omega=150$ and $Re_{cr}=3651.9$ are presented in Fig. 2. Here $-1.14\leqslant\psi_0\leqslant 15.72$, so that the secondary clockwise circulation is more than an order of magnitude smaller than the primary counterclockwise circulation driven by the surface tension variation at $r=1$. The counterclockwise circulation for $r<0.2$ is more than an order of magnitude smaller than the secondary circulation.

The mechanism which might make the combination of an RMF and system rotation more stabilizing than an RMF or rotation alone is the partial cancelation of the thermocapillary convection when the rotation of the feed rod and crystal produce the largest angular velocity at the liquid-solid interfaces, while the RMF in the opposite direction brakes the angular momentum, leading to a small or negative azimuthal velocity near $z=0$. Therefore, we consider two relatively large values of Re_Ω with Tm decreasing from zero to negative values corresponding to an RMF in the opposite azimuthal direction.

The values of Re_{cr} and λ_I for $Re_\Omega=100$ and $-5500<Tm<0$ are presented in Fig. 3. As Tm is decreased from zero, the addition of the RMF is clearly destabilizing. For the antisymmetric $m=2$ mode, Re_{cr} decreases from 2417.5 at $Tm=0$ to 2030.6 at $Tm=-625$, where the mode switches to an antisymmetric $m=1$ mode. As Tm decreases further, Re_{cr} decreases to a minimum of 1245.1 at $Tm=-1800$. At $r=1$ and $z=0$, $v_{\theta 0}$ first becomes negative at $Tm=-1200$, so that Re_{cr} does not reach its minimum until

the RMF has become strong enough to produce reverse azimuthal flow near $z=0$. There is a switch back to the antisymmetric $m=2$ mode at Tm$=-2604$ and Re$_{cr}=1696.3$. After this mode switch, Re$_{cr}$ decreases again, reaching a minimum of 1483.6 at $Tm=-3250$. As Tm decreases from -3250, Re$_{cr}$ increases monotonically as the magnitude and extent of the negative azimuthal velocity both increase. There is switch from the antisymmetric $m=2$ mode to the symmetric $m=2$ mode at Tm$=-3797$ and Re$_{cr}=1634$. At Tm$=-5500$, Re$_{cr}=2472.7$ for the symmetric $m=2$ mode, so that we have roughly returned to the Re$_{cr}=2417.5$ for Tm$=0$. The value of λ_I decreases as Tm is decreased from zero, except for a small increase just before the switch from the antisymmetric $m=1$ mode to the antisymmetric $m=2$ mode. At roughly Tm$=-3030$, λ_I becomes negative, so that the critical disturbance is propagating in the direction of the RMF rather than in the direction of the system rotation. For Re$_\Omega=100$, the extent and magnitude of the secondary clockwise meridional base-flow circulation for $z>0$ decreases as Tm is decreased from zero. The base-flow streamlines for Re$_\Omega=100$, $Tm=-5500$ and Re$_{cr}=2472.7$ are plotted in Fig. 4. The secondary circulation is very weak and is confined to a very small region near $r=0$, $z=1$, while the primary counterclockwise circulation closely resembles that for $Tm=$Re$_\Omega=0$. For Re$_\Omega=100$ and Tm$=-5500$, $-98.3\leqslant v_{\theta 0}\leqslant 100.0$, so that the RMF has produced a reverse azimuthal velocity with nearly the same maximum magnitude as that driven by the system rotation. The RMF produces an azimuthal body force which is distributed over the entire domain, while the effects of the system rotation arise from the viscous shear stresses at the liquid-solid interfaces. At the relatively large values of Re$_{cr}$, the effects of the viscous shear stresses at the liquid-solid interfaces do not extend far into the liquid, so that the RMF has a larger effect than the system rotation. For Re$_\Omega=100$, $Tm=-5500$ and Re$_{cr}=2472.7$, the $v_{\theta 0}=0$ line extends from $z=0.97$ at $r=1.0$ to $z=0.86$ at $r=0.5$, and then drops to $z=0.28$ at $r=0.0$. This drop near $r=0$ arises from the local downward convection of the positive angular momentum produced by the rotating solid at $z=1$. For this case, more than 80% of the liquid has a negative base-flow azimuthal velocity.

The values of Re$_{cr}$ and λ_I for Re$_\Omega=175$ and $-7000\leqslant$Tm$\leqslant 0$ are presented in Fig. 5. As Tm is decreased from zero, Re$_{cr}$ for the antisymmetric $m=2$ mode decreases from 4819.3 to a minimum of 1790.8 at Tm$=-4000$. The $v_{\theta 0}$ first becomes negative at $r=1$ and $z=0$ for Tm$=-2750$, so that there is again reverse flow before Re$_{cr}$ reaches its minimum. There is a switch from the antisymmetric $m=2$ mode to the antisymmetric $m=3$ mode at Tm$=-5000$ and Re$_{cr}=1995.8$, when the minimum $v_{\theta 0}$ is -66.3. For Tm$=-7000$, Re$_{cr}$ is 2297. As Tm is decreased for Re$_\Omega=175$, λ_I for the antisymmetric $m=2$ mode decreases monotonically from 417.59 for Tm$=0$ to 22.0 for Tm$=-5000$, and λ_I for the antisymmetric $m=3$ mode decreases monotonically from 42.39 for Tm$=-5000$ through zero at Tm$=-5850$ to -51.23 for Tm$=-7000$. Again $\lambda_I<0$ means that the critical disturbance propagates in the direction of the RMF.

For Re$_\Omega=175$, Tm$=-7000$ and Re$_{cr}=2297$, the base-flow streamlines and the lines of constant $v_{\theta 0}$ are plotted in Fig. 6. As Tm is decreased from zero, the primary counterclockwise circulation expands from that in Fig. 2 to occupy roughly $0.4<r<1.0$ in Fig. 6, while the secondary clockwise circulation is pushed into $0<r<0.4$. However, unlike Fig. 4 for Re$_\Omega=100$, the secondary flow is still significant for Re$_\Omega=175$ and Tm$=-7000$. Both circulations involve axially downward flow for $0.3<r<0.8$, and the associated convection of the positive azimuthal velocity produced by the system rotation alters the balance between the effects of system rotation and the RMF from that for Re$_\Omega=100$ and Tm$=-5500$. The $v_{\theta 0}=0$ line curves down from $z=0.96$ at $r=1.0$ to $z=0.25$ at $r=0.5$ and then curves up to $z=0.62$ at $r=0.0$. For this case, slightly more than half of the liquid has a negative azimuthal velocity.

4 Conclusions

The results presented here show that combining an RMF in one azimuthal direction with rotation of the crystal and feed rod in the opposite azimuthal direction leads to a thermocapillary instability for a smaller free-surface temperature difference than would be the case for either the rotation or the RMF alone. This indicates that the stabilizing effects of canceling part of the thermocapillary convection are overwhelmed by the destabilizing effects of reducing the average angular momentum. The partial cancelation of the thermocapillary convection does occur. For Re$_\Omega=100$, the maximum value of ψ_0 decreases from 13.14 for Tm$=0$ to a minimum of 8.32 at Tm$=-1600$ when $v_{\theta 0}=-18.8$ at $r=1$ and $z=0$, and then increases to 16.18 for Tm$=-5500$. For Re$_\Omega=175$, the maximum value of ψ_0 decreases from 18.9 for Tm$=0$ to a minimum of 9.43 for Tm$=-3500$ when $v_{\theta 0}=-47.8$ at $r=1$ and $z=0$, and then increases to 14.4 for Tm$=-7000$. However the destabilizing effects of the reduction of the average angular momentum are far greater than the stabilizing effects of the partial cancelation of the thermocapillary convection, so that this combination is not benefical.

Dold et al. [1] attributed the beneficial effects of the RMF to the increase of the frequency of the critical disturbance as the magnitude of Tm was increased. For both Re$_\Omega=100$ and Re$_\Omega=175$, the addition of the RMF in the opposite azimuthal direction decreases the value of λ_I. Therefore combining an RMF and system rotation in opposite azimuthal directions is also a bad idea because the frequency of the critical disturbance is less than that for either the RMF or system rotation alone.

Here we have only presented results for Pr$=0.02$, corresponding to molten silicon. There are important variations of the thermocapillary instability as Pr is varied over the small values for various semiconductors [6]. However the basic conclusion that combining rotating magnetic field and rotating system is not beneficial is certainly true for all molten semiconductors.

Acknowledgment

This research was supported by the National Science Foundation under Grant CTS-0129028 and by the National Aeronautics and Space Administration under Grants NAG 8-1705 and NAG 8-1817.

References

[1] Dold, P., Croll, A., Lichtensteiger, M., Kaiser, Th., and Benz, K. W., 2001, "Floating Zone Growth of Silicon in Magnetic Fields. IV. Rotating Magnetic Fields," J. Cryst. Growth, **231**, pp. 95–106.
[2] Walker, J. S., Martin Witkowski, L., and Houchens, B. C., 2003, "Effects of a Rotating Magnetic Field on the Thermocapillary Instability in the Floating Zone Process," J. Cryst. Growth, **252**, pp. 413–423.
[3] Wanschura, M., Shevtsova, V. M., Kuhlmann, H. C., and Rath, H. J., 1995, "Convective Instability Mechanisms in Thermocapillary Liquid Bridges," Phys. Fluids, **7**, pp. 912–925.
[4] Rupp, R., Muller, G., and Neumann, G., 1989, "Three-Dimensional Time Dependent Modelling of the Marangoni Convection in Zone Melting Configurations for GaAs," J. Cryst. Growth, **97**, pp. 34–41.
[5] Fischer, B., Friedrich, J., Weimann, H., and Muller, G., 1999, "The Use of Time-Dependent Magnetic Fields for Control of Convective Flows in Melt Growth Configurations," J. Cryst. Growth, **198/199**, pp. 170–175.
[6] Levenstam, M., Amberg, G., and Winkler, C., 2001, "Instabilities of Thermocapillary Convection in a Half-Zone at Intermediate Prandtl Number," Phys. Fluids, **13**, pp. 807–816.
[7] Dold, P., and Benz, K. W., 1999, "Rotating Magnetic Field: Fluid Flow and Crystal Growth Applications," Prog. Cryst. Growth Charact. Mater., **38**, pp. 7–38.
[8] Martin Witkowski, L., Walker, J. S., and Marty, Ph., 1999, "Nonaxisymmetric Flow in a Finite-Length Cylinder With a Rotating Magnetic Field," Phys. Fluids, **11**, pp. 1821–1826.
[9] Boyd, J. P., 2001, *Chebyshev and Fourier Spectral Methods*, 2nd ed., Dover Publications, New York.
[10] Smith, B. T. et al., 1976, *Matrix Eigensystem Routines—EISPACK Guide, Lecture Notes in Computer Science*, Vol. 6, New York, Springer-Verlag.
[11] Chen, G., Lizee, A., and Roux, B., 1997, "Bifurcation Analysis of the Thermocapillary Convection in Cylindrical Liquid Bridges," J. Cryst. Growth, **180**, pp. 638–647.